Supporting Information

UV-Emitting Upconversion-Based TiO_2 Photosensitizing Nanoplatform: Near-Infrared Light Mediated *in vivo* Photodynamic Therapy *via* Mitochondria-Involved Apoptosis Pathway

Zhiyao Hou,[†,§] Yuanxin Zhang,[†,§] Kerong Deng,[†,‡] Yinyin Chen,[†,‡] Xuejiao Li,[†,] Xiaoran Deng,[†,‡] Ziyong Cheng,[†] Hongzhou Lian,[†] Chunxia Li,[†,] and Jun Lin[†,]**

[†]State Key Laboratory of Rare Earth Resource Utilization

Changchun Institute of Applied Chemistry, Chinese Academy of Sciences,

Changchun 130022, P. R. China

[‡]University of Chinese Academy of Sciences, Beijing 100049, P. R. China

[§]These authors contributed equally

*Corresponding authors

E-mail: jlin@ciac.ac.cn (Prof. Jun Lin); cxli@ciac.ac.cn (Dr. Chunxia Li)

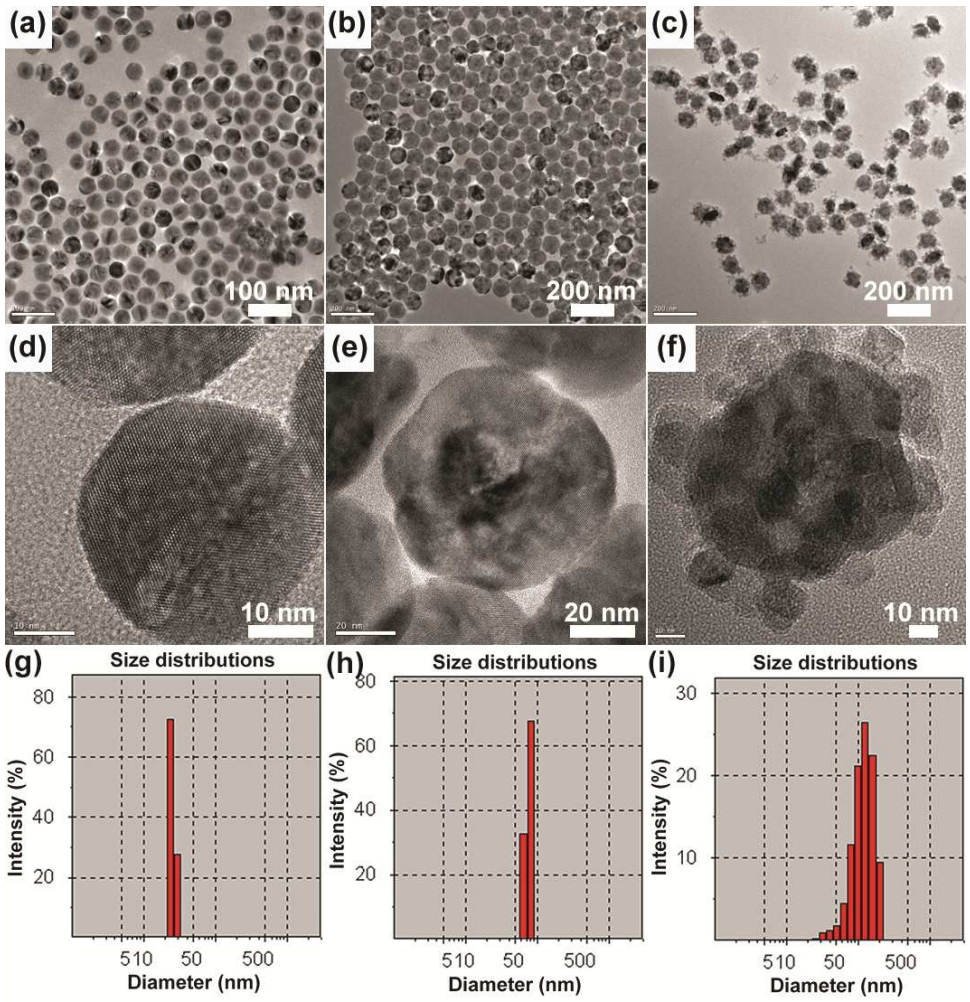

Figure S1 Low-magnification TEM images, high-resolution TEM (HRTEM) images and size distributions of original $NaYF_4:Yb^{3+},Tm^{3+}$ cores (a, d, g), $NaYF_4:Yb^{3+},Tm^{3+}$@ $NaGdF_4:Yb^{3+}$ core/shell UCNPs (b, e, h), and $NaYF_4:Yb^{3+},Tm^{3+}$@ $NaGdF_4:Yb^{3+}$@TiO_2 core/shell NCs (c, f, i).

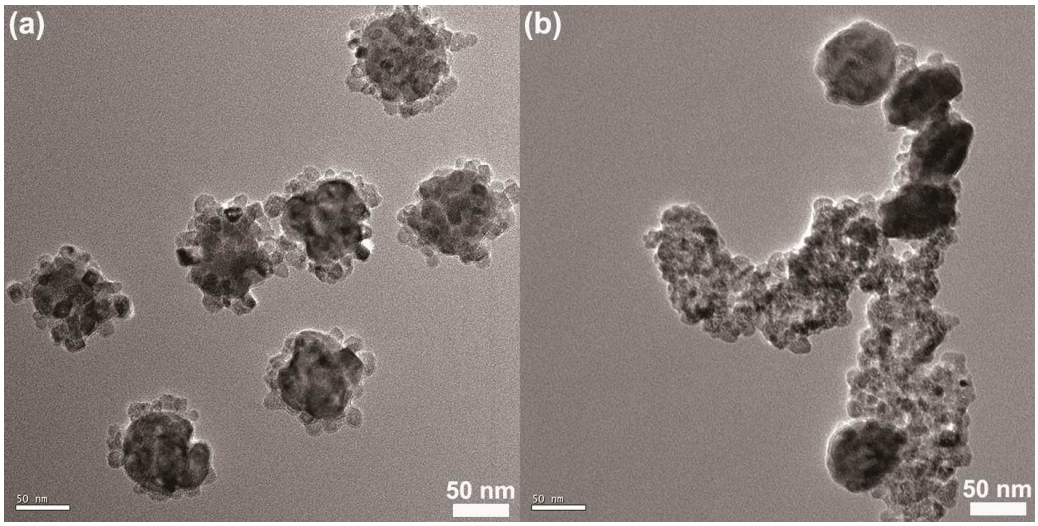

Figure S2 TEM image of the $NaYF_4:Yb^{3+},Tm^{3+}$@ $NaGdF_4:Yb^{3+}$@TiO_2 core/shell NCs synthesized with (a) and without PVP (b).

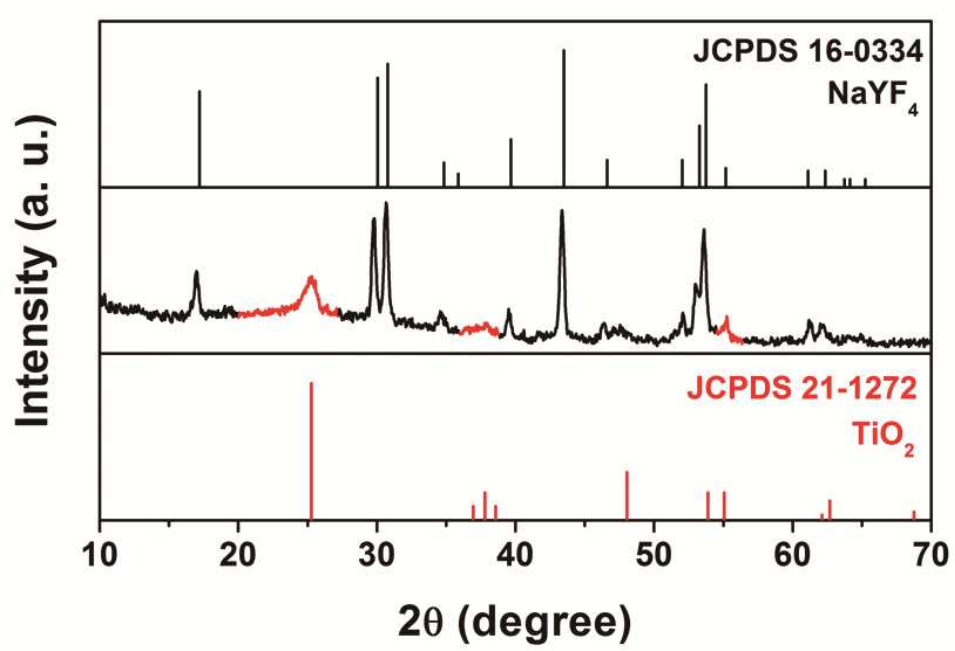

Figure S3 XRD pattern of $NaYF_4$:Yb^{3+},Tm^{3+}@ $NaGdF_4$:Yb^{3+}@TiO_2 core/shell NCs.

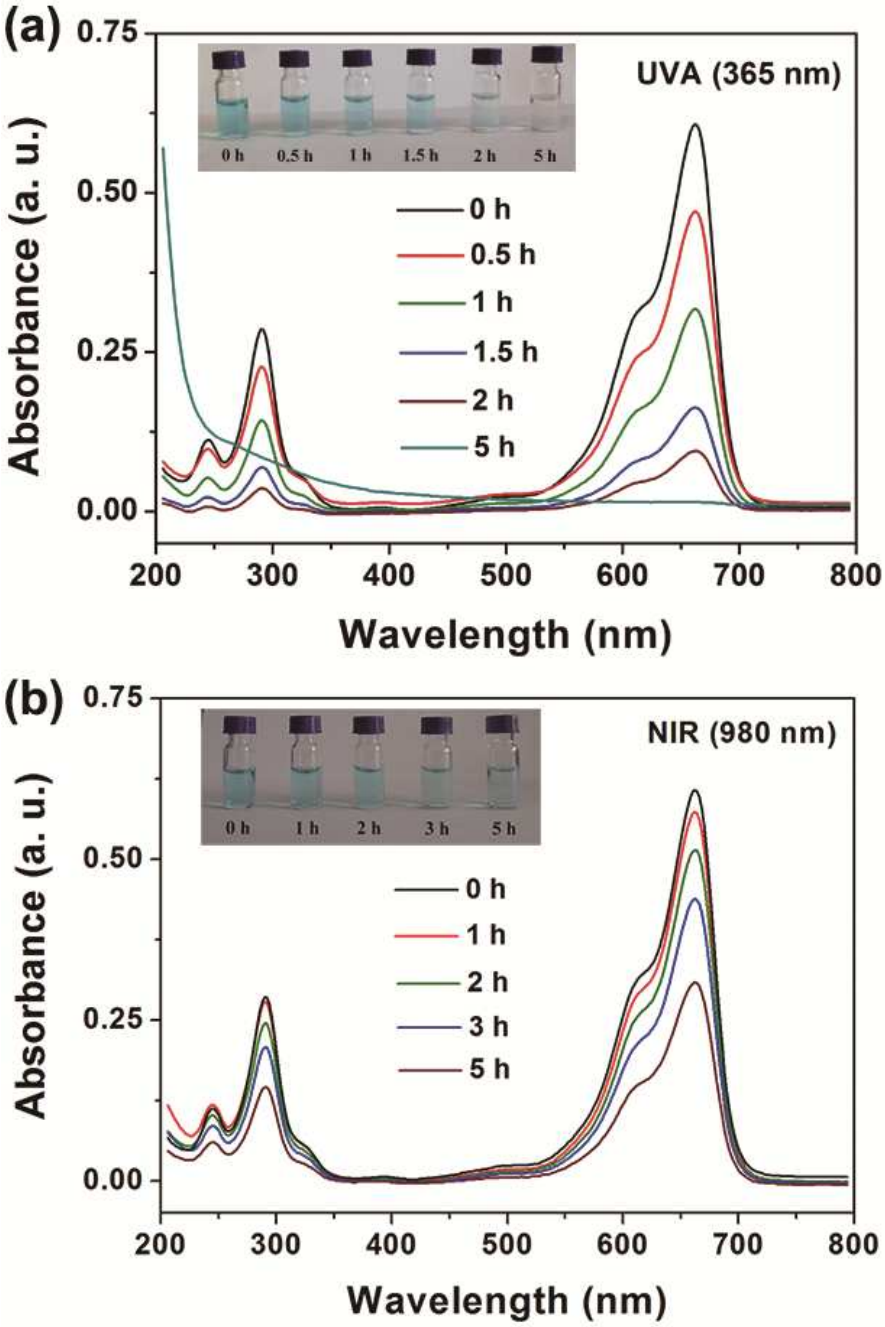

Figure S4 Variation in absorbance spectra of MB catalyzed by UCNPs@TiO_2 NCs as a function of the irradiation time under 365 nm UV light (a) and 980 nm NIR laser (b) excitation (inset: digital photographs of MB solution after irradiation).

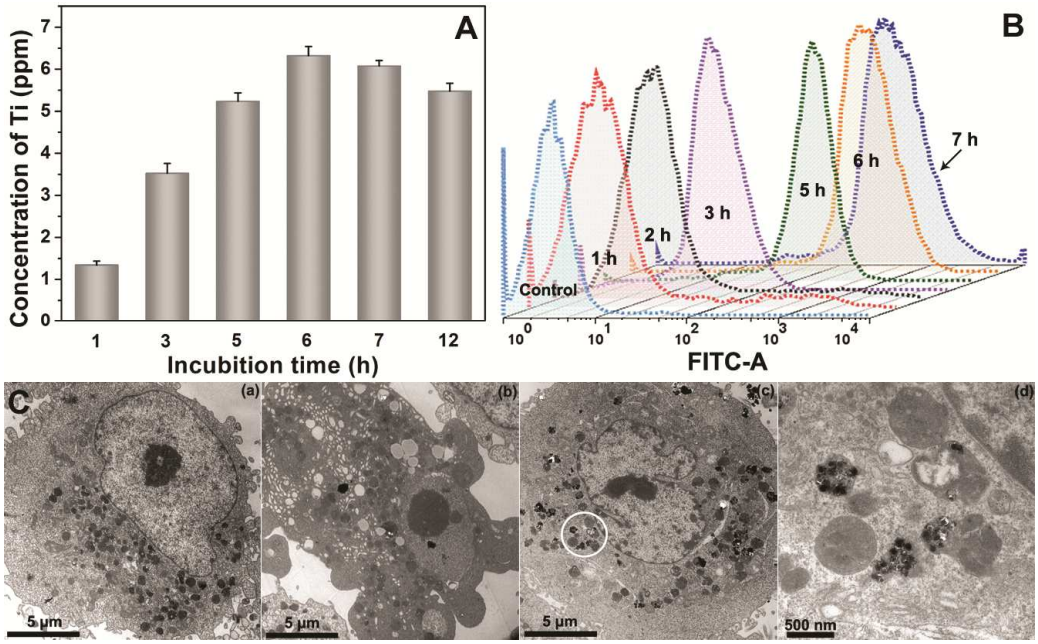

Figure S5 ICP-MS (A) and FCM (B) analyses of Hela cells incubated with UCNPs@TiO_2 for various times. TEM images (C) of blank control cell (a), Hela cell incubated with UCNPs@TiO_2 NCs (500 μg·mL^{-1}, 6 h incubation) under 980 nm NIR laser irradiation (b), Hela cell incubated with UCNPs@TiO_2 NCs without 980 nm NIR laser irradiation (c, d).

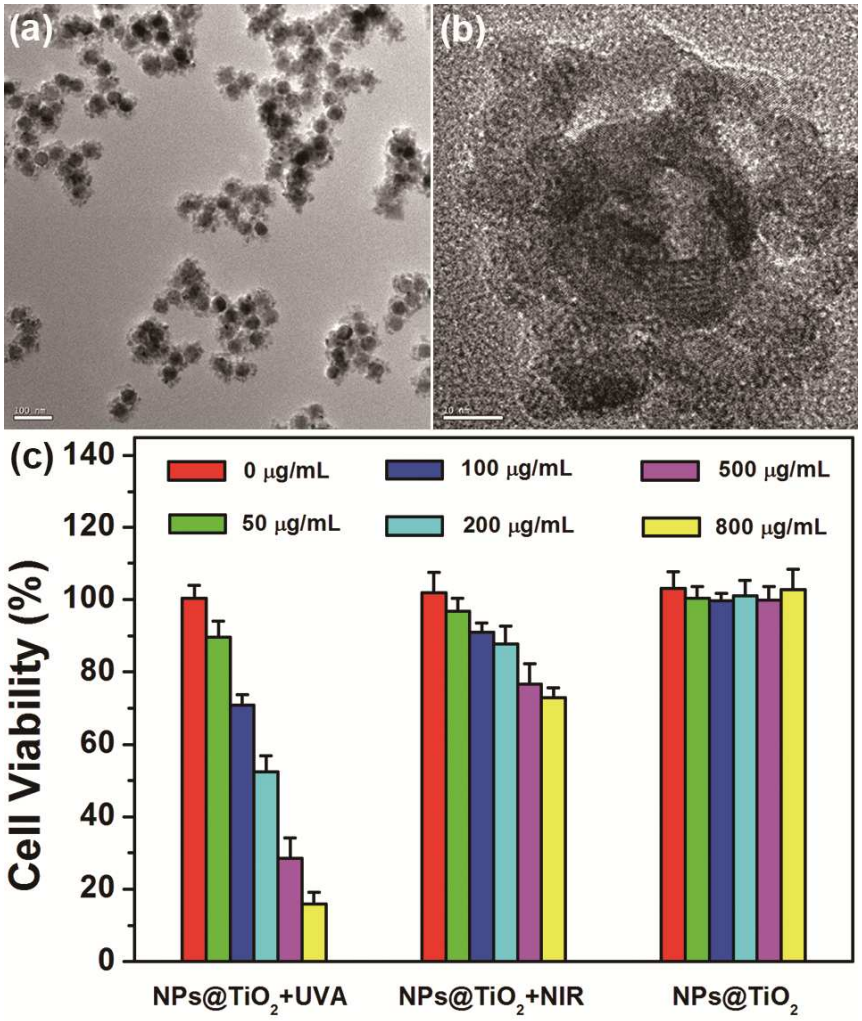

Figure S6 TEM (a) and HR-TEM (b) images of $NaYF_4:Yb^{3+},Tm^{3+}@TiO_2$. *In vitro* viabilities of Hela cells treated with $NaYF_4:Yb^{3+},Tm^{3+}@TiO_2$ under 365 nm UV light irradiation, 980 nm NIR laser irradiation and non-irradiation (c). Error bars indicate standard deviations, n = 3.

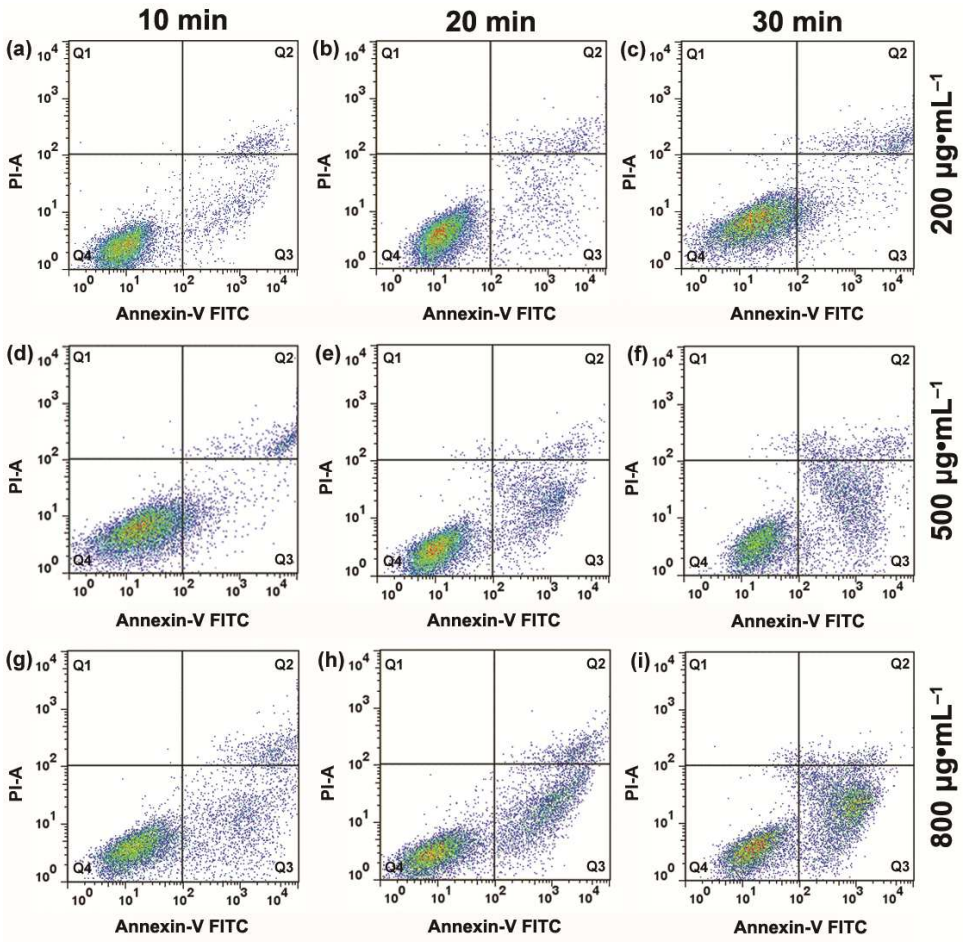

Figure S7 Apoptosis of Hela cells by staining with Annexin V-FITC and PI after NIR light mediated PDT treatment with various concentrations (200, 500, and 800 $\mu g \cdot mL^{-1}$) and irradiation times (10, 20, and 30 min).

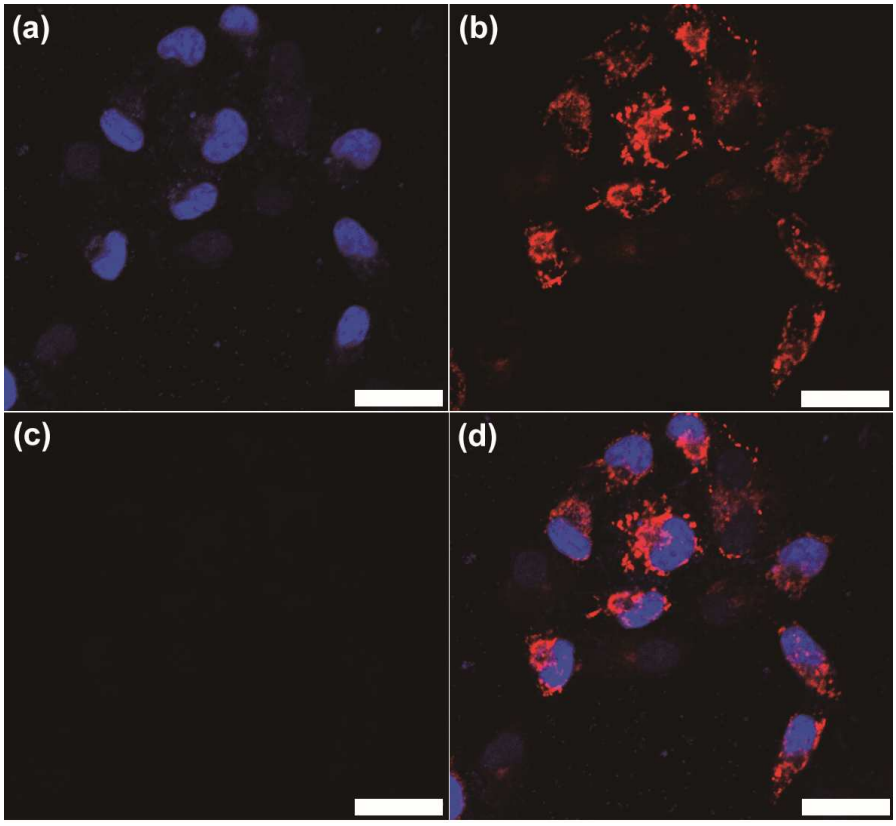

Figure S8 Control cells treated with UCNPs@TiO_2 NCs alone and stained with JC-1(red fluorescence), the nuclei of cells being dyed in blue by Hoechst 33324 (a), JC-1 forms red-emitting aggregates in the mitochondrial matrix (b), green-emitting monomers in cytoplasm (c), the overlapped image (d). All scale bars are 30 μm.

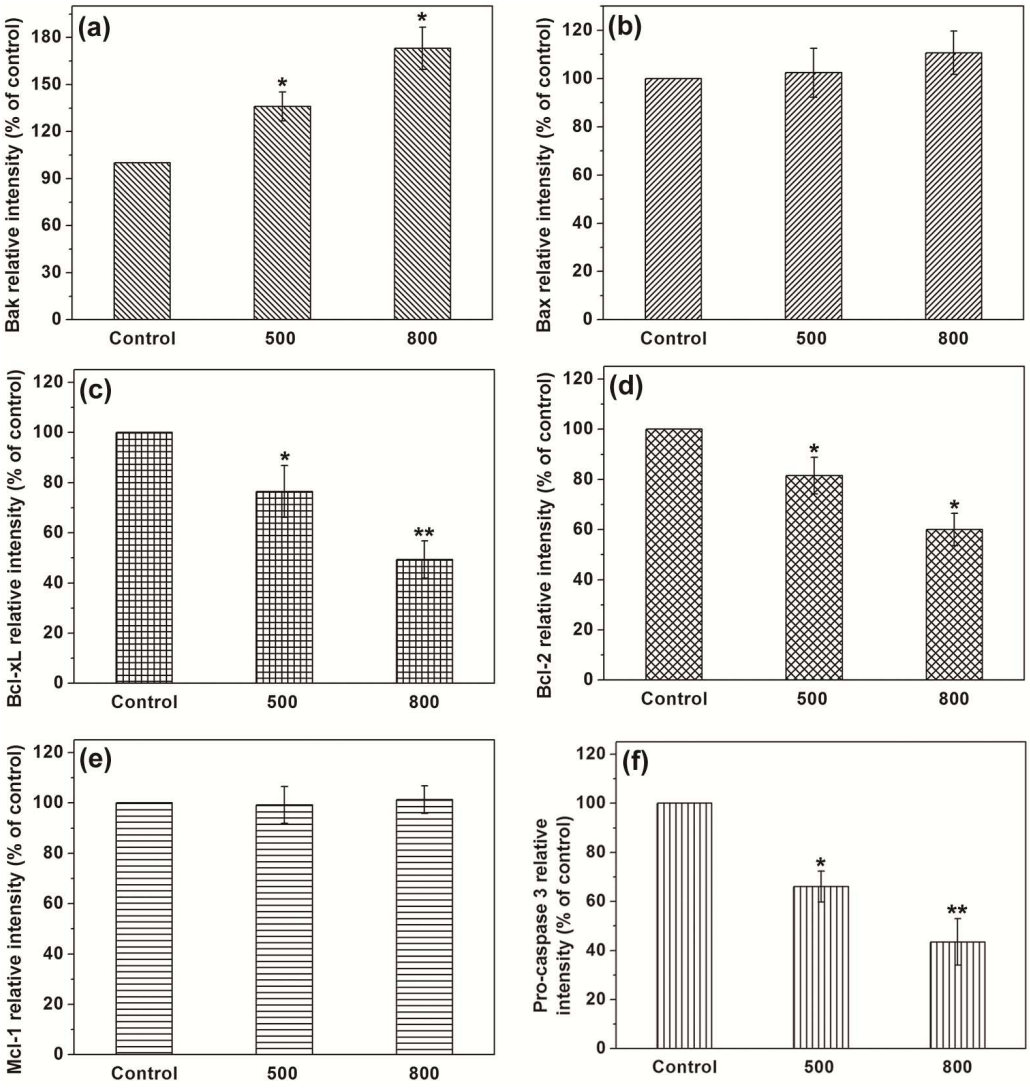

Figure S9 Representative immunohistochemical staining quantitative analysis of Bak (a), Bax (b), Bcl-xL (c), Bcl-2 (d), Mcl-1 (e) and Pro-caspase 3 (f) expression. After normalization with the corresponding GAPDH expression, the protein expression levels were determined using densitometry scans to obtain quantitative data. Untreated cells were used as control. The data are representative of three independent experiments. The data are expressed as the mean ± standard deviation (n = 3). **P*<0.05 or ***P*<0.01 as compared with the control group.

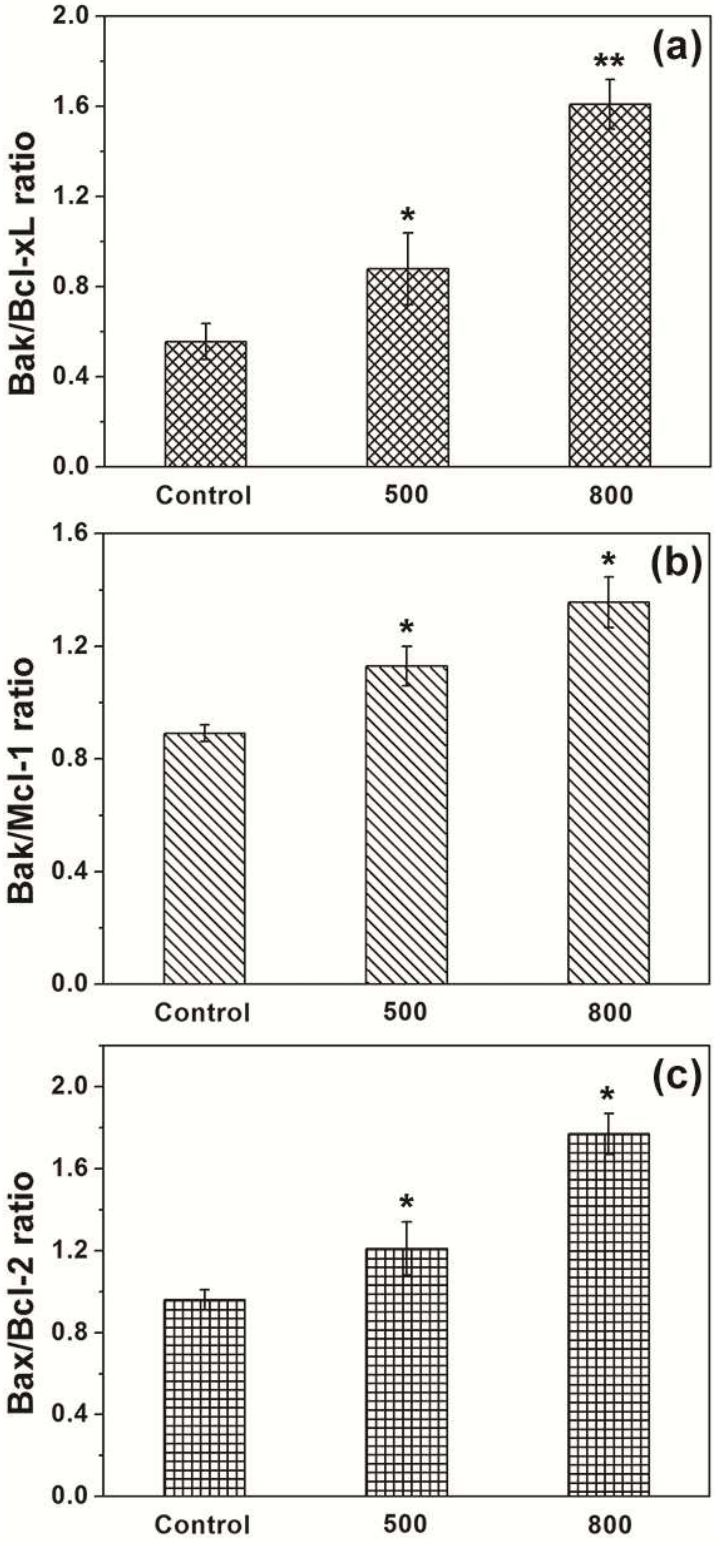

Figure S10 The ratios of Bak/Bcl-xL, Bak/Mcl-1 and Bax/Bcl-2. **P*<0.05 or ***P*<0.01 as compared with the control group.

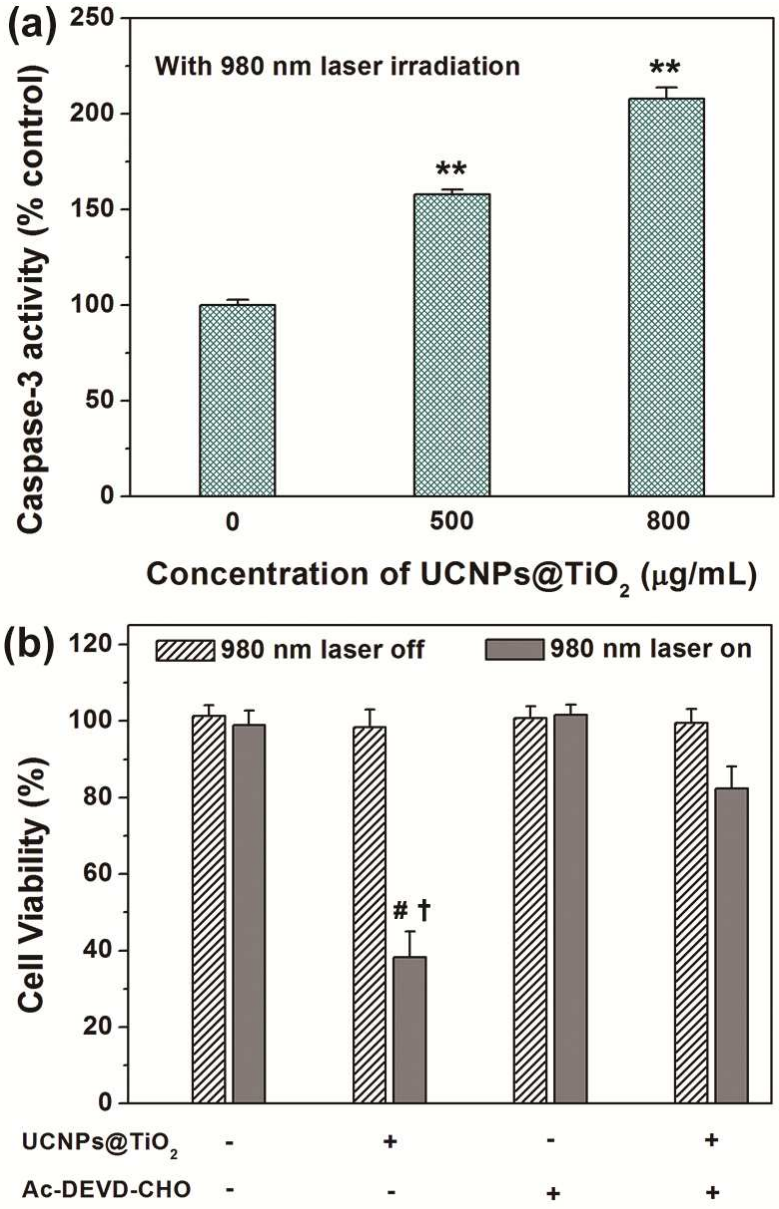

Figure S11 Effect of NIR-mediated PDT on caspase 3 activity in Hela cells (a). The Hela cell survival after NIR-mediated PDT treatment with caspase-3 inhibitor (b). Hela cells were pretreated with 50 μM of Ac-DEVD-CHO for 1 h, and then incubated with UCNPs@TiO_2 via 980 nm laser irradiation. The cell survival was determined by the MTT assay. Results are presented as mean ± standard deviation (n = 3). $^{**}P<0.01$ as compared with the control group. $^{\#}P<0.01$ as compared with the control group. $^{\dagger}P<0.01$ as compared with the Ac-DEVD-CHO added PDT group.

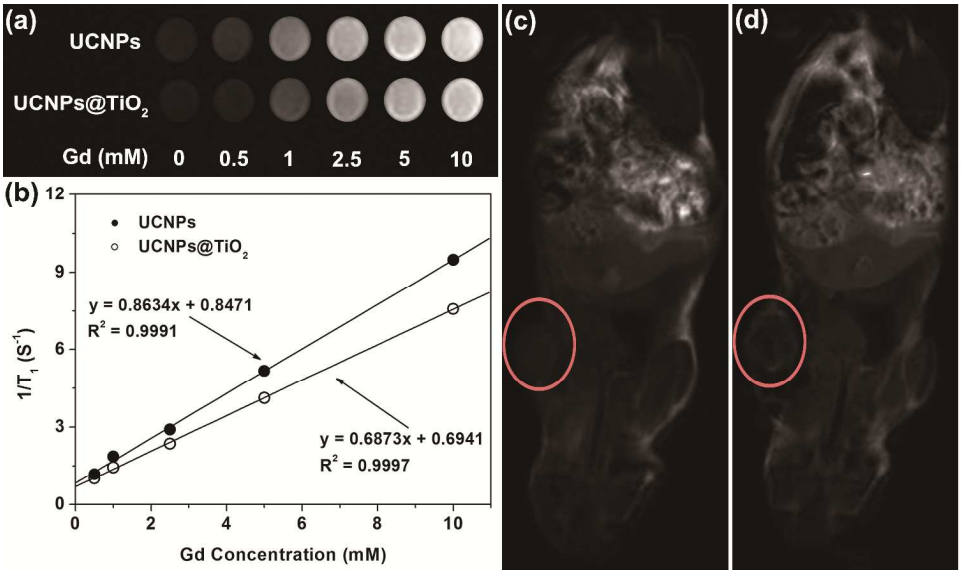

Figure S12 T_1-weighted MR images of UCNPs and UCNPs@TiO_2 with various Gd^{3+} concentrations (a). Relaxation rate r_1 ($1/T_1$) versus different mass concentrations of UCNPs and UCNPs@TiO_2 at room temperature using a 1.2 T MRI scanner (b). T_1-weighted MR images of a tumor-bearing Balb/c mouse: preinjection (c) and after injection of UCNPs@TiO_2 *in situ* (d).

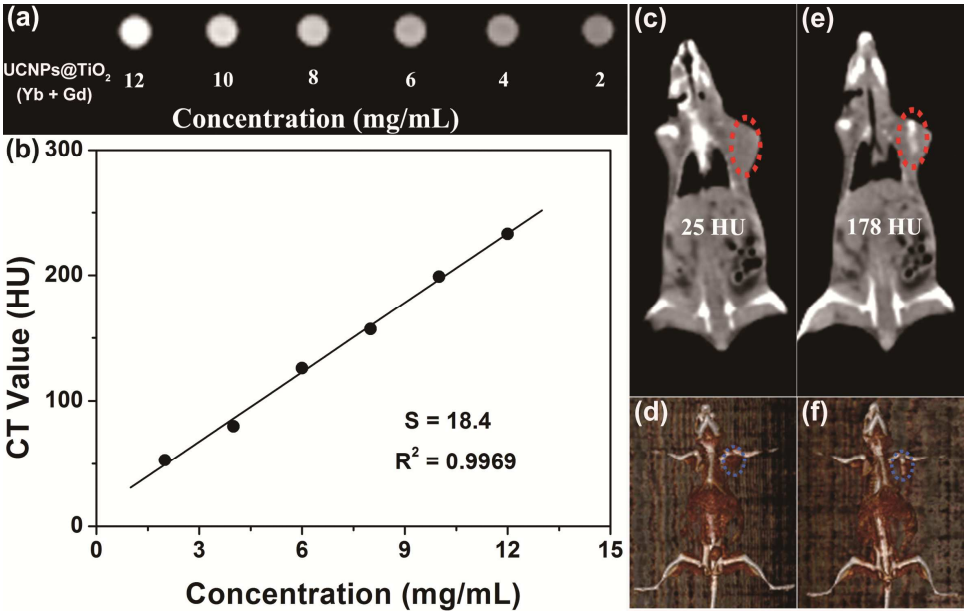

Figure S13 (a) *In vitro* CT phantom images of UCNPs@TiO_2 with different concentrations. (b) HU value of aqueous solution of UCNPs@TiO_2 NCs. *In vivo* CT phantom and 3D-rendering images of a tumor-bearing Balb/c mouse intratumorally pre-injection (c, d) and post-injection (e, f).

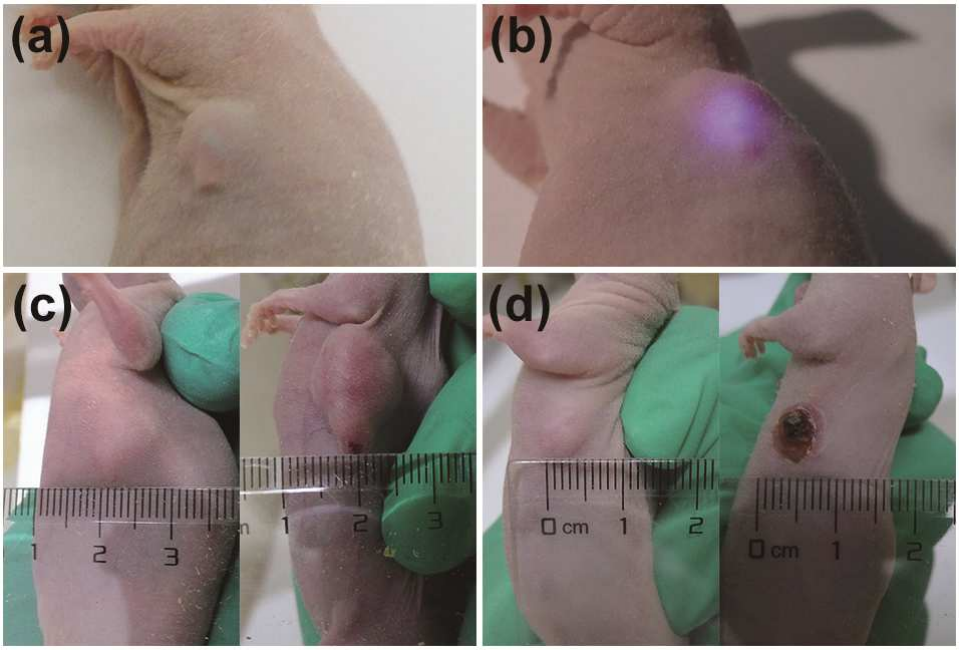

Figure S14 *In vivo* PDT through 980 nm NIR laser irradiation (a), up-conversion luminescence can be observed after the intratumoral injection of UCNPs@TiO_2 NCs via 980 nm laser (b). Digital photographs of tumor sections after cancer therapy form control group (c) and PDT group (d).

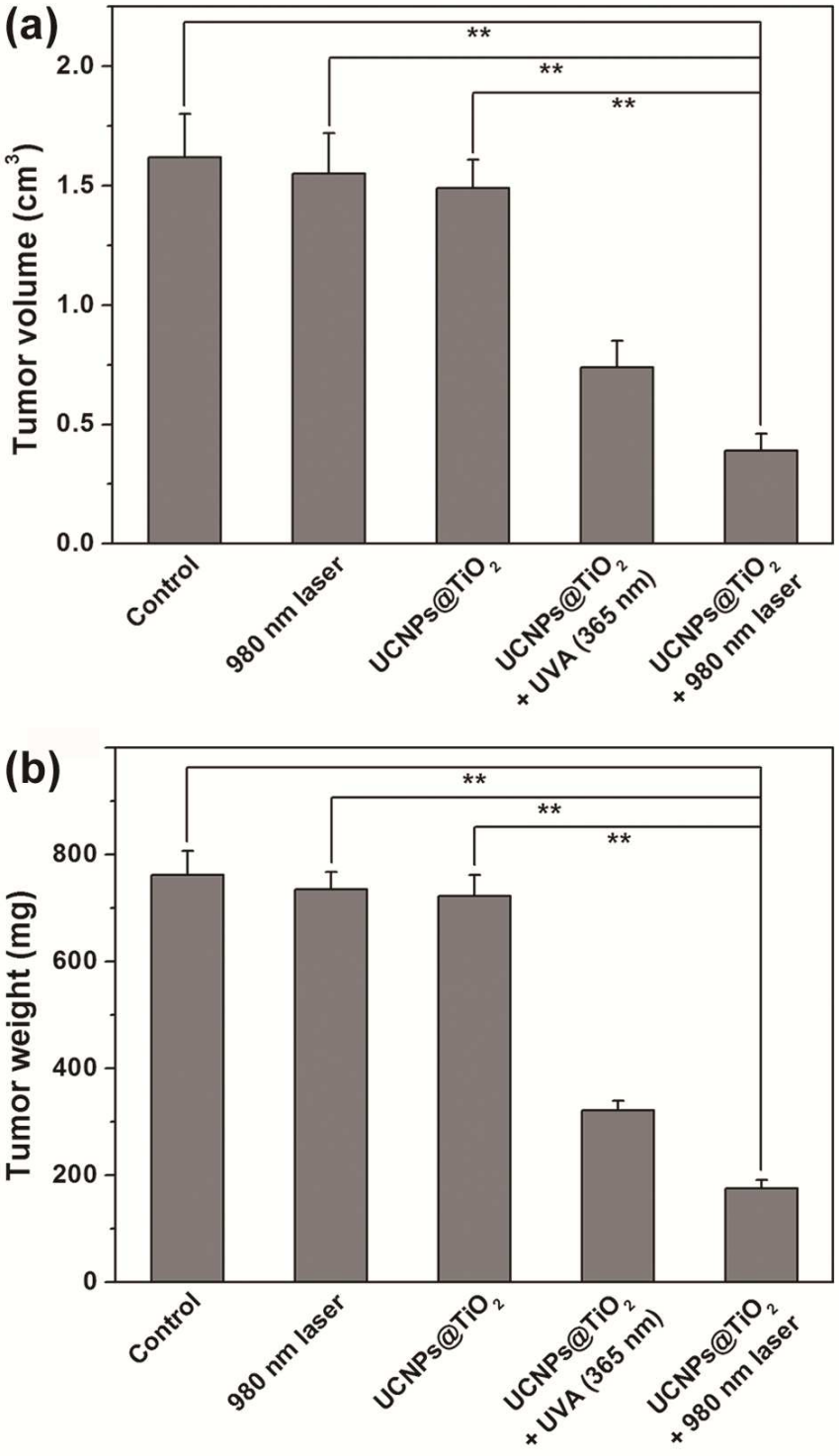

Figure S15 Tumor volumes (a) and weights (b) of the excised tumors from mice in each group at the last day of experiment. Error bars indicate standard deviations, n = 6. Three asterisks indicate statistically significant discrepancy (**P<0.01 as compared with the control group).

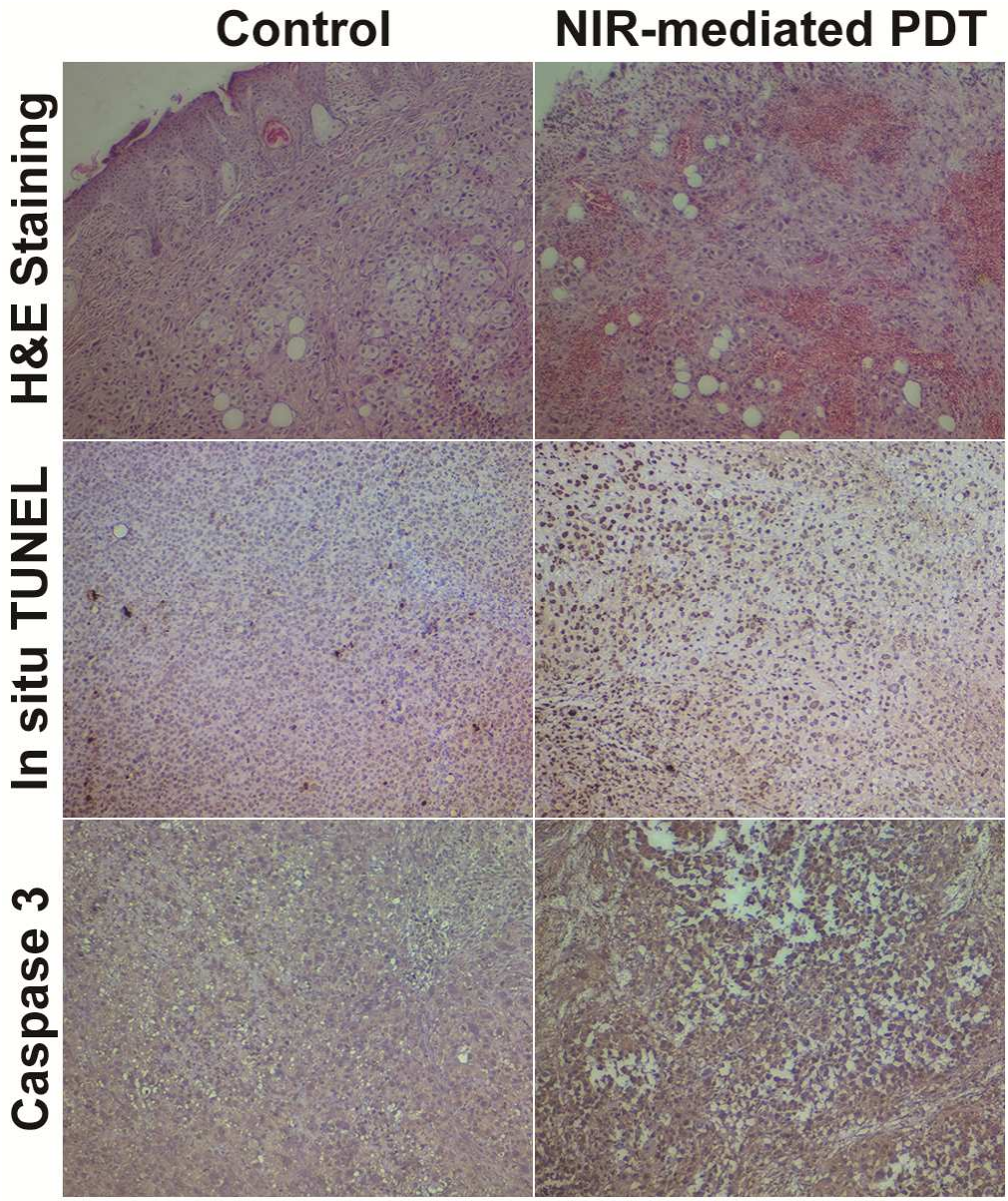

Figure S16 Representative images with low-magnification of the tumor sections examined by H&E staining (A), TUNEL assay (B) and immunohistochemical staining for caspase 3 (C). (Original magnification: A, B and C, 80×)